

Yields and isomeric ratio of xenon and krypton isotopes from thermal neutron fission of ^{235}U

S. S. Hsu, J. T. Lin, C. M. Yang, and Y. W. Yu

College of Nuclear Science, National Tsing-Hua University, Hsinchu, Taiwan, Republic of China

(Received 4 March 1980)

The experimental cumulative yields of $^{85}\text{Kr}^m$, ^{87}Kr , ^{88}Kr , $^{133}\text{Xe}^g$, $^{135}\text{Xe}^m$, and $^{135}\text{Xe}^g$ and the independent isomeric yield of $^{133}\text{Xe}^m$ in the thermal neutron fission of ^{235}U have been measured by the gas chromatographic method. The independent yields of $^{133}\text{Xe}^g$, $^{135}\text{Xe}^m$, and $^{135}\text{Xe}^g$ were deduced with the aid of ^{133}I and ^{135}I data. The isomeric yield ratios of ^{133}Xe and ^{135}Xe have been computed and compared with theoretical values since they have the same high spin state $J = 11/2^-$ and low spin ground state $J = 3/2^+$. The influence of the shell effect on the fission isomeric yield ratio is discussed. From the measured independent yield of Xe isotopes plus the reported data, the Xe-isotopic distribution curve has been constructed. The curve is compared with the isotopic distribution curves of Xe isotopes formed in 11.5 GeV proton interactions with ^{238}U and Cs isotopes formed in 24 GeV proton interactions with ^{238}U . Upon fitting the yield curves we find that only those products with $N/Z \geq 1.48$ fit a curve typical of a binary fission process.

NUCLEAR REACTIONS ^{235}U (thermal neutron fission) $^{85}\text{Kr}^m$, ^{87}Kr , ^{88}Kr , $^{133}\text{Xe}^g$, $^{133}\text{Xe}^m$, and $^{135}\text{Xe}^g$ cumulative yields, $^{133}\text{Xe}^m$, $^{135}\text{Xe}^g$, $^{135}\text{Xe}^m$, and $^{135}\text{Xe}^g$ independent yields and isomeric ratio.

I. INTRODUCTION

The experimental measurement of the fission yield of xenon and krypton nuclides by the gas chromatographic technique,^{1,2} and the mass spectroscopic method^{3,4} have been reported. However, the independent yields of both isomeric and ground states of ^{133}Xe and ^{135}Xe have not been well known. The values are especially interesting because they have the same high spin state $J = \frac{11}{2}^-$ and low spin state $J = \frac{3}{2}^+$. The influence of the $N=82$ shell closure on the fission isomeric yield ratio could be directly observed from the experimental data. On the other hand, they are located in the down wing of the Xe-isotopic distribution curve for thermal neutron fission of ^{235}U . A comparison with the Xe-isotopic distribution curve formed in 11.5 GeV proton interactions with ^{238}U ,³ would certify which products were formed by the binary fission process. This helps to clarify some unknown mechanism in the more complex high energy process which has been the subject of recent interest.⁵

In the present work, the cumulative yield of some radioactive krypton and xenon nuclides and independent isomeric yield of ^{133}Xe and ^{135}Xe from thermal neutron fission of ^{235}U have been measured by the activation plus the gas chromatographic method. The independent yield of xenon isotopes with reported data were used to construct the Xe-isotopic distribution curve from thermal neutron fission of ^{235}U and the curve was compared with the Xe-isotopic distribution curve from 11.5 GeV protons with ^{238}U (Ref. 3) and the Cs-isotopic dis-

tribution curve from 24 GeV protons with ^{238}U (Ref. 6) as discussed in Sec. IV.

II. EXPERIMENTAL

A metallic sample of about 40 mg of natural uranium was used for irradiation. The uranium chip was cleaned with 6*N* HNO_3 and various solvents, vacuum dried, weighted and sealed in a quartz tube capsule.

The samples were irradiated by means of the pneumatic tube system of the Tsing-Hua Open-pool Reactor (THOR) at full power (1 MW) with thermal neutron flux of about 2×10^{12} $n/\text{sec cm}^2$ for 2 min to 60 min according to the half-life of isotopes to be determined.

A. Separation procedure

After irradiation, the uranium samples were transferred into a bottle (B) as shown schematically in Fig. 1. The solution containing 1 ml conc. HNO_3 , 1 ml conc. HCl , and 0.5 ml I-carrier solution were added to (B) through funnel (C). Adjustment of the valve (A) allows a carrier gas flow at constant rate and the system pressure is kept at about 500 mm Hg. As the uranium starts to dissolve rapidly the nitrogen carrier gas bubbles through the sample solution and then carries the volatile gas through the AgNO_3 solution [in (D)] where I and Br were removed. Next a dry bed [column (E)] which contains KOH , CuO , CaCO_3 , and silica gel removes moisture and acid fumes. Finally, the carrier gas with dried Kr and Xe

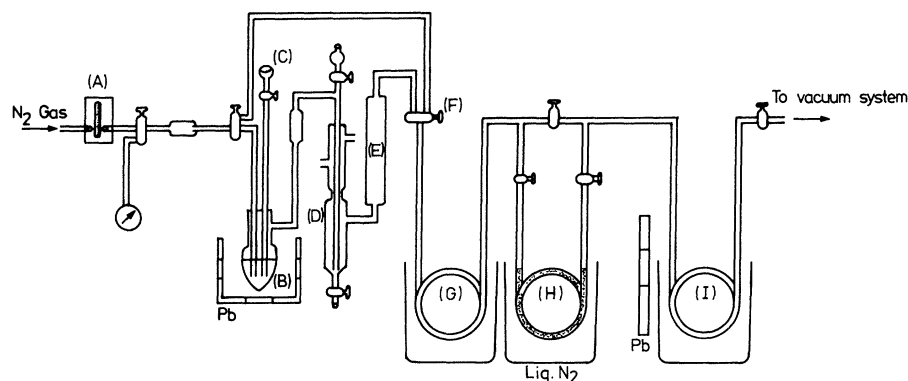


FIG. 1. Apparatus for Kr and Xe absorption.

passed through column (H) which contained active charcoal cooled to liquid nitrogen temperature.

B. Radioactivity measurements

The growth activity was measured with NaI(Tl) detectors fit into coils (G) and (I). After the maximum counting rate had been reached, column (H) was isolated and γ spectra were measured with a calibrated Ge(Li) detector in conjunction with a 4096 channel analyzer and HP-2100 computer system for data acquisition. Table I summarizes the decay properties on which our measurement was based and identifies the source of this information.⁷

C. Efficiency and calibrations

The Ge(Li) detector efficiency has been calibrated with the known absolute disintegration rate γ standard sources obtained from the National Bureau of Standards and New England Nuclear.

The efficiency of column (H) was measured in the following way. After column (H) (with collected Kr and Xe) was removed, a new charcoal column (H) was inserted (in liquid nitrogen tempera-

ture). The decay products of $^{135}\text{I} \rightarrow ^{135}\text{Xe}$ were collected for about 6 h from the flow of N_2 carrier gas. Then we counted the 9.1 h, 250 keV γ peak in column (H) and the 6.5 h, 1.260 MeV γ peak in column (D). The result shows not only that the absorption is complete but also that the yield is close to 100%.

As the whole system's actual chemical yield is still not known, all our results are normalized to $^{85}\text{Kr}^m$. We believe the error from chemical yield should be less than 5%.

III. RESULTS

The activities of each γ peak were analyzed and extrapolated to the time at the end of the bombardment or to the time of separation by the CLSQ computer program⁸ and then converted to disintegration rates by means of the radiation abundances and counting efficiencies. The yield which has been determined to be very near 100% in column (H), the counting geometry, and neutron flux were treated as a common factor that was determined by assuming the known cumulative fission yield required, in all cases, corrections for growth and decay of parent-daughter separation. These corrections and the decay chains used for calculation of ^{133}Xe and ^{135}Xe isomeric yields will be given in further detail in a separate section.

A. Fission yields

The measured fission yields are tabulated in Table II with quoted uncertainties which are standard deviations based on the agreement between replicates. All the values are normalized to the $^{85}\text{Kr}^m$ cumulative yield of 1.33% from Ref. 9, which experimental error estimates at about $\pm 12\%$. The cumulative yield of ^{87}Kr , ^{88}Kr , ^{133}Xe , and ^{135}Xe are very close to the chain yield.

Since the time elapsed from the end of irradiation

TABLE I. Decay properties of observed nuclides (Ref. 7).

Nuclide	Half-life	Observed ray (keV)	Abundance (per 100 decays)
$^{85}\text{Kr}^m$	4.48 h	151	78
^{87}Kr	76 min	403	50
^{88}Kr	2.84 h	196	26
$^{133}\text{Xe}^m$	2.19 d ^a	233	14
$^{133}\text{Xe}^g$	5.29 d ^a	81	37
$^{135}\text{Xe}^m$	15.7 min ^b	527	80
$^{135}\text{Xe}^g$	9.14 h	250	92 ^b

^a E. A. Henry, Nucl. Data Sheets 11, 495 (1974).

^b E. A. Henry, Nucl. Data Sheets 14, 191 (1975).

TABLE II. Fission yield of some Kr and Xe isotopes.

Isotopes	Number of determinations	Present results		Previously measured fission yields ^a (%)
		Type of yield	Fission yield (%)	
⁸⁵ Kr ^m	5	C	1.33 ^b	1.33
⁸⁷ Kr	5	C	3.39 ± 0.42	2.37
⁸⁸ Kr	5	C	3.74 ± 0.45	3.64
¹³³ Xe ^m	2	I	0.12 ± 0.06	
¹³³ Xe ^g	2	I	0.34 ± 0.18	
¹³³ Xe	2	C	7.21 ± 0.85	6.77
¹³⁵ Xe ^m	3	I	0.034 ± 0.010	
¹³⁵ Xe ^m	3	C	1.01 ± 0.15	1.05
¹³⁵ Xe ^g	3	I	0.75 ± 0.12	
¹³⁵ Xe	3	C	7.07 ± 0.85	6.72

^aReference 9.^bNormalized to the cumulative fission yield of ⁸⁵Kr^m given in Ref. 9.

tion to the time of target dissolution is 15 min or longer, no decay correction for ⁸⁵Kr^m is necessary. The decay chain and genetic relationship used to obtain independent yields of ¹³³Xe^m and ¹³³Xe^g are based on Ref. 10, from which we know ¹³³I decays to the ¹³³Xe^m state only 2.4% while 97.5% decays to the ground state with a half-life of 20.8 h. In these runs the target was irradiated 5 min with a waiting time of about 4 h before chemistry. The contribution from decay of 20.8 h ¹³³I with a cumulative yield of 6.75% (Ref. 9) is used for successive decay corrections. The 55.4 min ¹³³Te^m is assumed to decay to ¹³³I. To obtain independent yields of ¹³⁵Xe^m and ¹³⁵Xe^g, the genetic relationship is based on Ref. 11. The 6.7 h ¹³⁵I decays 15.5% to the isomeric state and 84.5% to the ground state. The internal γ -ray transition to the ¹³⁵Xe ground state is 75%.¹¹ The growth decay correction contributed to the measured activities of the precursors during the irradiation and the subsequent decay to the time at the maximum growth counting rate of the absorption column was determined by a NaI(Tl) detector.

From Table II we can see that almost all the cumulative yields measured in this work are in good agreement with previously reported values except for ⁸⁷Kr, which has a cumulative yield of 3.39 ± 0.42%. This is higher than the reported value of 2.37% and it could be due to the use of the older 403 keV γ abundance, 84% in Ref. 9.

B. Isomeric yield ratio

The isomeric yield ratios of ¹³³Xe and ¹³⁵Xe obtained from independent yields are listed in Table III. The large discrepancy between runs is quite possibly due to a large correction in the decay factors that lead to large error flags. The isomeric yield ratio of ¹³⁵Xe, lower than ¹³³Xe by a factor of 7.8, could be due to the $N=82$ shell effect to be discussed in Sec. IV B.

C. Xe-isotopic yield distribution

The measured ¹³³Xe and ¹³⁵Xe total independent yields are 0.46 ± 0.18 and 0.79 ± 0.15 respectively, in combination with independent yields of ¹³⁷Xe through ¹⁴³Xe measured by Ehrenberg and Amiel⁴ and listed in Table IV. From these values we can construct a Xe-isotopic yield distribution curve as a function of N/Z as shown in Fig. 2. The distribution is a Gaussian-like curve with a maximum around ¹³⁸Xe. The Gaussian parameters were obtained by fitting the experimental values with a nonlinear least-square program by the expression

$$Y_1(Z) = Y_{\max} \exp[-(Z - Z_p)^2]/2\sigma^2,$$

where Z_p is most probable charge, σ is the width parameter, and Y_{\max} is the maximum yield of the Gaussian. The resulting isotopic distribution curve is shown by the solid curve across the ex-

TABLE III. Isomeric yield ratios of ¹³³Xe and ¹³⁵Xe.

Nuclide	High spin state	Low spin state	$Y_{\text{high}}/Y_{\text{low}}$
¹³³ Xe	$J = \frac{11}{2}^-$	$J = \frac{3}{2}^+$	0.35 ± 0.19
¹³⁵ Xe	$J = \frac{11}{2}^-$	$J = \frac{3}{2}^+$	0.045 ± 0.012

TABLE IV. The independent yield of Xe isotopes from thermal neutron fission of ^{235}U .

Isotopes	Independent yield % present work	Independent yield % (Ref. 4)
^{133}Xe	0.46 ± 0.18	
^{135}Xe	0.78 ± 0.15	
^{136}Xe		(2.0)
^{137}Xe		$2.97^{+0.4}_{-0.32}$
^{138}Xe		$5.03^{+0.62}_{-0.50}$
^{139}Xe		$5.16^{+0.50}_{-0.40}$
^{140}Xe		$2.92^{+0.43}_{-0.31}$
^{141}Xe		$1.19^{+0.19}_{-0.13}$
^{142}Xe		$0.63^{+0.10}_{-0.07}$
^{143}Xe		$0.27^{+0.08}_{-0.07}$

perimental data in Fig. 2 and the Gaussian parameters are summarized in Table V, column two.

IV. DISCUSSION

A. Xe-isotopic yield distribution curves

Assuming the unchanged charge distribution (UCD) hypothesis, we express the isotopic distribution in terms of the $A = 138$ charge dispersion curve (CDC) with the same Z_p and Y_{\max} based on unchanged charge density of compound nucleus and fragment calculated by the procedure of Ref. 12. The parameters obtained are listed in Table V. The second column is the Gaussian obtained by best fit of the Xe-isotopic distribution data. The third column gives the Gaussian of $A = 138$ CDC with fixed Z_p and Y_{\max} computed by the procedure of Ref. 11. The fourth column is the best fit Gaussian of the experimental $A = 138$ charge dispersion data, which is taken from Ref. 13. All three Gaussians together with the measured Xe-data are plotted on Fig. 2. From it we can see that the width parameter σ of the Xe-isotopic

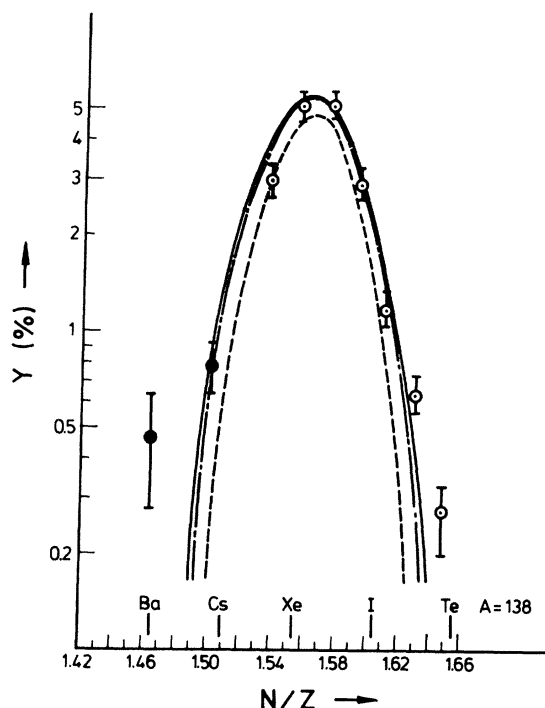


FIG. 2. Xe-isotopic yield distribution curve. The solid points are from our measurements, the open points are from Ref. 4, and the solid line represents a Gaussian fit to the data. The dot-dashed curve is $A = 138$ CDC obtained by the procedure of Ref. 12. The dashed curve is the Gaussian fit to the experimental CD data.

distribution is 0.65 ± 0.08 which is greater than 0.59 ± 0.06 obtained from $A = 138$ CDC and 0.50 ± 0.05 obtained from experimental $A = 138$ CDC. The mass yield obtained from the Xe-isotopic distribution curve is 8.79 ± 1.04 and from the $A = 138$ charge dispersion curve is 8.24 ± 0.85 . The experimental value of the $A = 138$ mass yield is 6.80 ± 0.17 .¹²

Now we plot this curve and normalize the Y_{\max} to the Xe-isotopic yield distribution curve for the interaction of 11.5 GeV protons with ^{238}U (Ref. 3) and also the Cs-isotopic yield distribution curve

TABLE V. Gaussian parameters of Xe-isotopic yield distribution curve.

	Xe-isotopic distribution	$A = 138$ charge dispersion ^a from Xe isotopic distribution	$A = 138$ charge dispersion ^b experimental
Y_{\max} (%)	5.57 ± 0.10	5.57	5.05 ± 0.05
Z_p	53.90 ± 0.20	53.90	53.84 ± 0.05
N/Z_p	1.56 ± 0.01	1.56 ± 0.01	1.56 ± 0.01
$\sigma(Z)$	0.63 ± 0.08	0.59 ± 0.06	0.50 ± 0.06
Y_A (%)	8.78 ± 1.04	8.24 ± 0.85	6.80 ± 0.17

^a At fixed Y_{\max} and Z_p CDC obtained by the process of Ref. 12.

^b Fit the experimental charge dispersion data from Ref. 13 with mass yield: $A = 138$, $Y_A = 6.80 \pm 0.017$ (%). Fractional yield: ^{52}Te , 0.03 ± 0.01 ; ^{53}I , 0.18 ± 0.08 ; ^{54}Xe , 0.74 ± 0.08 ; ^{55}Cs , 0.047 ± 0.002 .

for the interaction of 24 GeV protons with ^{238}U . This is shown on Fig. 3 with quite interesting results. Here we have assumed charge independence on the nuclear process and also have neglected the three mass units difference between the target nuclides ^{235}U and ^{238}U , because we are sure that the yield of Xe isotopes from the interaction of thermal neutrons with ^{235}U is purely from a binary fission process. Now it is apparent that only at the far end ($N/Z > 1.48$ of the neutron excess part were the high energy products formed from binary fission.

B. Isomeric yield ratios

The isomeric yield ratios of ^{113}Xe and ^{135}Xe from thermal neutron fission of ^{235}U are listed in Table III. According to the statistical model the probability distribution of levels $P(J)$ is a function of J which can be expressed as¹⁴

$$P(J) \propto (2J+1) \exp[-(J+\frac{1}{2})^2/2B^2],$$

where B is a parameter related to the moment of inertia and the temperature of the excited fission fragments. Since ^{133}Xe and ^{135}Xe both have the same high spin $J = \frac{11}{2}^-$ isomeric state and low spin $J = \frac{3}{2}^+$ ground state, the ratio of the populations of the high spin to low spin states should be equal. The decrease of the isomeric yield ratio of ^{135}Xe by a factor of 7.8 from ^{133}Xe could be purely due to the shell effect. A similar case of ^{131}Te and ^{133}Te have the same high spin $J = \frac{11}{2}^-$ states and low spin $J = \frac{3}{2}^+$ ground states as Xe. Therefore, the calculated isomeric yield ratio is 0.78 (Ref. 15) for both isotopes, but the observed ratios are 1.90 ± 0.4 for ^{131}Te and 1.33 ± 0.11 for ^{133}Te by Ref. 16 and 1.8 ± 0.4 for ^{131}Te and 1.55 ± 0.5 for ^{133}Te by Ref. 17. The authors¹⁶ conclude that as the number of neutrons of the products approaches the neutron magic number 82, the isomeric yield ratio will decrease with a trend which is lower than our experimental results.

V. CONCLUSION

The cumulative fission yields of six krypton and xenon nuclides have been measured. They

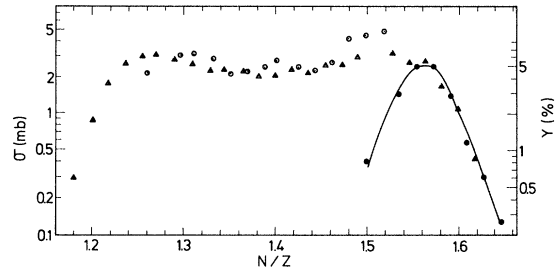


FIG. 3. Independent yields of xenon nuclides from the fission of ^{235}U with thermal neutrons (solid points) and from the interaction of ^{238}U with high energy protons (open points).

show good agreement with previous published data.⁹ Four independent fission yields of ^{133}Xe and ^{135}Xe ground and isomeric states have also been determined. Since their high spin states and low spin states both have $J = \frac{11}{2}^-$ and $\frac{3}{2}^+$, respectively, we believe the decrease of the isomeric yield ratio by a factor of 7.8 could be due to the 82 neutron shell effect.

The Xe isotopic yield distribution curve constructed by the measured independent yield of ^{133}Xe and ^{135}Xe plus the published data of ^{136}Xe through ^{143}Xe shows a Gaussian-like distribution. The curve also has been compared with the isotopic yield distribution curves of Xe and Cs produced from GeV proton bombardment of ^{238}U . It shows only those yields on the far neutron excess side ($N/Z = 1.48$ to 1.66) which fit the curve of thermal neutron fission of ^{235}U .

ACKNOWLEDGMENTS

We would like to thank the operating group of the Tsing-Hua Nuclear Reactor for its assistance in sample irradiation, and also gratefully acknowledge the assistance of the Isotope Division for providing the counting facilities. This work was supported by the National Science Council under Contract No. NSC-69E-0413.

¹J. Hudis, T. Kirshen, R. W. Stoennes, and O. A. Schaefer, Phys. Rev. C **1**, 2019 (1970).

²J. H. Forster, N. T. Porile, and L. Yaffe, Can. J. Chem. **44**, 2951 (1966).

³Y. W. Yu, N. T. Porile, R. Warasila, and O. A. Schaefer, Phys. Rev. C **8**, 1091 (1973).

⁴B. Ehrenberg and S. Amiel, Phys. Rev. C **6**, 618 (1972).

⁵Y. W. Yu, Phys. Rev. C **22**, 933 (1980).

⁶J. Chaumont, Ph.D. thesis, University of Paris, 1970

(unpublished).

⁷Table of Isotopes, edited by C. M. Lederer and V. S. Shirley, 7th ed. (Wiley, New York, 1978).

⁸J. B. Cumming, Annu. Rev. Nucl. Sci. **13**, 261 (1963).

⁹M. E. Meek and B. F. Rider, G. E. Report NEDO-12154 (1972).

¹⁰S. Spiridon, J. Inorg. Nucl. Chem. **35**, 713 (1973).

¹¹H. Fenerstein and J. Oschinski, Inorg. Nucl. Chem. Lett. **12**, 243 (1976).

- ¹²A. C. Wahl, R. L. Ferguson, D. R. Nethaway, D. E. Troutner, and K. Wolfsberg, Phys. Rev. 126, 1112 (1962).
- ¹³S. Amiel and H. Feldstein, Phys. Rev. C 11, 845 (1975).
- ¹⁴J. B. Wilhelmy, E. Cheifetz, R. C. Jared, S. G. Thompson, H. R. Bowman, and J. O. Rasmussen, Phys. Rev. C 5, 2041 (1972).
- ¹⁵H. Warhanek and R. Vandenbosch, J. Inorg. Nucl. Chem. 26, 669 (1964).
- ¹⁶N. Imanishi, I. Fujiwara, and T. Nishi, Nucl. Phys. A 263, 141 (1976).
- ¹⁷D. G. Sarantites, G. E. Gordon, and C. D. Coryell, Phys. Rev. 138B, 353 (1965).